Submitted to ApJL

Self-shielding Effects on the Column Density Distribution of Damped Lyman Alpha Systems

Zheng Zheng & Jordi Miralda-Escudé

Department of Astronomy, The Ohio State University, Columbus, OH 43210

zhengz@astronomy.ohio-state.edu, jordi@astronomy.ohio-state.edu

ABSTRACT

We calculate the column density distribution of damped Lyα systems, modeled as spherical isothermal gaseous halos ionized by the external cosmic background. The effects of self-shielding introduce a hump in this distribution, at a column density $N_{HI} \sim 1.6 \times 10^{17} X^{-1}\,\mathrm{cm}^{-2}$, where X is the neutral fraction at the radius where self-shielding starts being important. The most recent compilation of the column density distribution, by Storrie-Lombardi & Wolfe, shows marginal evidence for the detection of this feature due to self-shielding, suggesting a value $X \simeq 10^{-3}$. Assuming a photoionization rate $\Gamma \simeq 10^{-12}\,\mathrm{s}^{-1}$ from the external ionizing background, the radius where self-shielding occurs is inferred to be $\sim 3.8\,\mathrm{kpc}$. If damped Lyα systems consist of a clumpy medium, this should be interpreted as the typical size of the gas clumps in the region where they become self-shielding. Clumps of this size with typical column densities $N_H \sim 3 \times 10^{20}\,\mathrm{cm}^{-2}$ would be gravitationally confined at the characteristic photoionization temperature $\sim 10^4$ K if they do not contain dark matter. Since this size is similar to the overall radius of damped Lyα systems in Cold Dark Matter models, where all halos are assumed to contain similar gas clouds producing damped absorbers, this suggests that the gas in damped absorbers is in fact not highly clumped.

Subject headings: galaxy: formation – quasars: absorption lines

1. INTRODUCTION

Damped Lyα systems (hereafter, DLAs) contain most of the atomic hydrogen in the universe (e.g., Wolfe et al. 1995; Storrie-Lombardi & Wolfe 2000). They are therefore fundamental objects to understand galaxy formation: in the process of forming galaxies, the matter that is originally in the low-density, ionized intergalactic medium must invariably become first atomic, before it can form molecular clouds and stars.

The nature and geometrical shape of the DLAs is still a subject of debate. The two alternative hypotheses that are being discussed at present and confronted with the observations are as follows: (a) They are rotating disks, which may or may not be forming stars; (b) They are approximately spherical halos, where global rotation contributes little to the support against gravity. The truth may be a combination of these two possibilities: DLAs might be described as flattened halos or thick disks, with a range of the ratio of rotation velocity to velocity dispersion.

A fundamental property of DLAs is that their associated metal lines reveal the presence of multiple absorbers in most of the systems, which are thought to arise from clumps of gas. The multiple absorption lines appear over velocity intervals of 30 to 300 $\mathrm{km\,s^{-1}}$. The statistical properties of the multiple absorption lines have been used to attempt to distinguish between the disk and halo models, but both alternatives seem to be consistent with observations (Prochaska & Wolfe 1997, 1998; Haehnelt, Steinmetz, & Rauch 1998, 2000; McDonald & Miralda-Escudé 1999). Although the observations reveal that there are usually one or a few clumps intersected along a random line of sight, with characteristic column densities of $\sim 10^{20}\,\mathrm{cm^{-2}}$, the size of the clumps is not well known. Constraints in a few systems from double lines of sight in lensed QSO's, and from model calculations of the ionization parameter, indicate sizes or structure in the range of 20 pc to 1 kpc (Rauch, Sargent, & Barlow 1999; López et al. 1999). Models of structure formation predict that the overall size of DLAs is of the order of 1 to 10 kpc (e.g., Katz et al. 1996; Gardner et al. 1997; McDonald & Miralda-Escudé 1999). If the clump size is not much smaller than the size of DLAs, then the absorption lines would actually be arising from mild fluctuations in density and velocity in a turbulent medium; whereas if the clump sizes are much smaller, they would be real separate entities with a large overdensity relative to an interclump medium.

This paper discusses the effects of self-shielding on the form of the column density distribution of damped Lyα systems, and the dependence of this distribution on the size of the gas clumps. As the gas becomes self-shielding against the external cosmic ionizing background, there is a rapid transition from ionized to fully atomic gas, and this causes a feature in the column density distribution. If X is the neutral fraction of the gas seen at a column density $N_{HI} = 1.6 \times 10^{17}\,\mathrm{cm^{-2}}$ (where the optical depth to photons at the hydrogen ionization edge is equal to one), a hump in the column density distribution will occur at $N_{HI} \sim 1.6 \times 10^{17} X^{-1}\,\mathrm{cm^{-2}}$. Therefore, a measurement of X from this feature in the column density distribution, combined with an independent estimate of the ionizing background intensity, can be used to infer the size of the gas clumps.

Observationally, compared with the expected number extropolated from low column density distributions, an excess of absorption systems with $N_{HI} \gtrsim 2 \times 10^{20}\,\mathrm{cm^{-2}}$ is found by Lanzetta et al. (1991). The recent compilation of the column density distribution of known DLAs by Storrie-Lombardi & Wolfe (2000) shows more clearly a hump around $N_{HI} \sim 2 \times 10^{20}\,\mathrm{cm^{-2}}$. Theoretically, based on an approximate calculation of the self-shielding effect, Murakami & Ikeuchi (1990) showed that a flat part appears in the column density distribution. With a simplified consideration on the ionizing flux transfer, Petitjean, Bergeron, & Puget (1992) investigated models of self-gravitating, photoionized, spherical gaseous cloud and explained the flattening of the column density distribution

at $N_{HI} \sim 2 \times 10^{20}\,\mathrm{cm}^{-2}$ as the effect of self-shielding. Similar calculations of the expected column density distribution due to self-shielding have been done by Corbelli, Salpeter, & Bandiera (2001) for plane-parallel geometry.

Here, we will consider a spherical geometry with a singular isothermal profile to perform a self-shielding calculation, and focus on the application of inferring the size of the gas clumps in damped Lyα systems.

2. METHOD

2.1. Model for Gaseous Halos

We model a DLA as a spherical cloud of gas with a singular isothermal profile, $\rho_g = A/r^2$, with a cutoff at the virial radius, where ρ_g is the gas density. The model depends only on the constant A, which can be recast in terms of the mass of an associated virialized dark matter halo. We will be presenting results for dark matter halo masses of 10^9, 10^{10}, 10^{11}, and $10^{12} M_\odot$, assuming that 5% of the mass of the halo is in the form of gas. For the cosmological model with $\Omega = 1$, $H_0 = 70\,\mathrm{km\,s^{-1}\,Mpc^{-1}}$, and at $z = 3$, the virial radii corresponding to these halo masses are $r_{\rm vir} = 5.2, 11.1, 23.9$, and $51.5\,\mathrm{kpc}$, and the halo circular velocities are $V_c = 29, 62, 134$, and $289\,\mathrm{km\,s^{-1}}$, respectively (e.g., Padmanabhan 1993). In Cold Dark Matter models of structure formation, the damped Lyα systems should be located in halos over this range of masses (e.g., Gardner et al. 1997). The constant A is simply determined by the condition that 5% of the halo mass is equal to the total gas mass within radius $r_{\rm vir}$. The model ignores clumpiness of the gas, but as discussed later the results depend only on the assumed radius at a given density, so the halo radius will essentially play the role of the radius of a clump.

2.2. The Background Spectrum And The Ionization Profiles

The other quantity that determines the profile of neutral hydrogen is the intensity of the external ionizing background. We assume an intensity of $I_\nu = 3 \times 10^{-22}\,\mathrm{erg\,cm^{-2}\,s^{-1}\,Hz^{-1}\,sr^{-1}}$, constant at all frequencies between the H I Lyman limit, ν_L, and the He II Lyman limit, $4\nu_L$. The intensity is set to zero at frequencies above $4\nu_L$. This is a sufficiently good approximation for our purpose to the background spectrum expected from QSOs, after absorption by the Lyα forest is taken into account (e.g., Haardt & Madau 1996). The reason is that He II becomes self-shielding at a larger radius in the gaseous halo than H I (owing to the faster He II recombination rate and the lower intensity of the cosmic background at the He II Lyman limit, compared to hydrogen; e.g., Miralda-Escudé & Ostriker 1990), and therefore the photons at frequency above $4\nu_L$ in the cosmic background are absorbed before reaching the region where H I opacity is important. With this spectrum, our adopted value of the intensity at the H I Lyman limit corresponds to a

H I photoionization rate $\Gamma = 1.25 \times 10^{-12}\,\mathrm{s}^{-1}$.

In our calculation, we will set the total hydrogen number density to $n_H = 0.76\rho_g/m_H$ (where m_H is the mass of the hydrogen atom), and the electron number density to $n_e = 0.82(1 - x_{HI})\rho_g/m_H$, where $x_{HI} = n_{HI}/n_H$ is the hydrogen neutral fraction. The factors 0.76 and 0.82 assume a helium abundance of $Y = 0.24$ by weight, and that all the helium is in the form of He I and He II with the same neutral fraction as hydrogen. Other than these factors, the presence of helium is ignored in our calculation. This is a good enough approximation owing to the small helium abundance by number, plus the fact that every photoionization of He I produces a photon following recombination of He II which ionizes hydrogen.

2.3. Self-shielding Calculation

We compute the self-shielded H I density profile using an iterative procedure similar to the one described by Tajiri & Umemura (1998). Photoionization equilibrium demands that at each radius, we have

$$x_{HI}(r) \int_{4\pi} d\Omega \int_{\nu_L}^{\infty} \frac{I_{\nu,0} e^{-\tau_\nu}}{h\nu} a_\nu d\nu = [1 - x_{HI}(r)]^2 \, \frac{0.82\rho_g(r)}{m_H} \, \alpha_B(T) \ , \tag{1}$$

where $x_{HI}(r)$ is the hydrogen neutral fraction at radius r, $I_{\nu,0}$ is the cosmic background intensity, τ_ν is the photoionization optical depth from radius r to infinity along a given direction, a_ν is the photoionization cross section of hydrogen, and $\alpha_B(T)$ is the case B recombination coefficient at temperature T (we use the on-the-spot approximation, see Osterbrock 1989). We fix the temperature to 2×10^4 K, for which the recombination coefficient is $\alpha_B = 1.41 \times 10^{-13}\,\mathrm{cm}^3\,\mathrm{s}^{-1}$ (Spitzer 1978; Verner & Ferland 1996). One can compute self-consistently the gas temperature assuming thermal equilibrium under photoionization conditions, but in practice the gas is likely to be frequently shock-heated in any model of moving gas clumps in a halo. To numerically evaluate the integral in equation (1), we compute the integral over frequency at many values of the optical depth and obtain a fit to this function. The integral over solid angle is reduced to one dimension in the spherical case, and is performed at each radius. We initiate $x_{HI}(r)$ by assuming the system to be optically thin. At each iteration, τ_ν is recomputed for each radius and polar angle, and new values of x_{HI} are found. This iteration is repeated until x_{HI} has converged with a fractional error less than 10^{-5}.

3. RESULTS

The neutral fraction profile as a function of radius, in kpc, is shown in the left panel of Figure 1 for the four halo masses. As expected, the ionizing photons penetrate deeper in halos of lower mass. For a power-law density profile, self-similarity implies that the shape of the x_{HI} profile depends on the gas density and the background intensity only through one parameter, X, which is the neutral

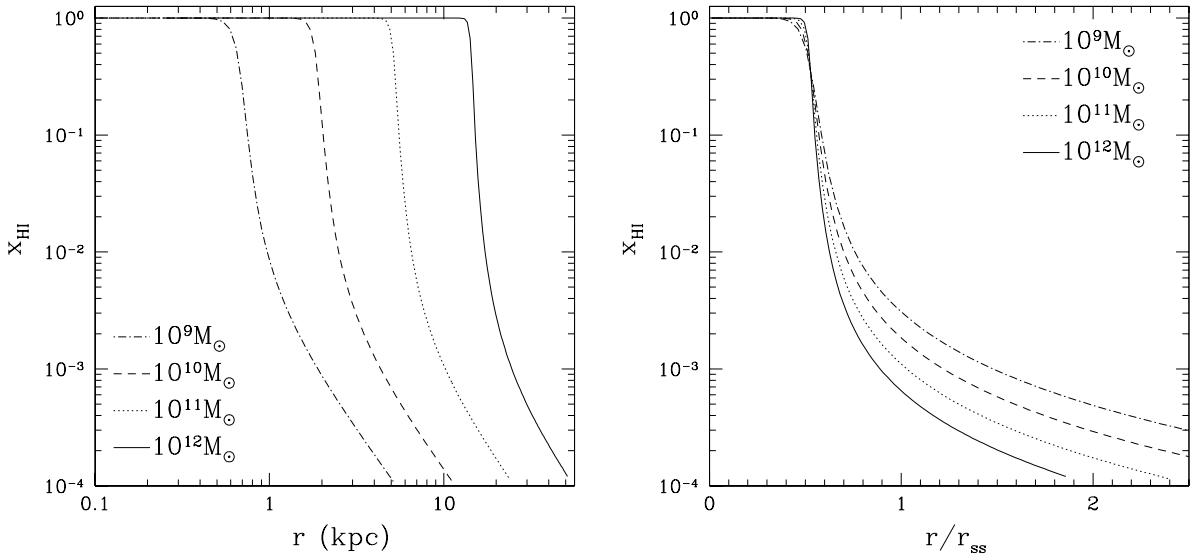

Fig. 1.— The neutral fraction profile as a function of radius for four halo masses. As explained in the text, these x_{HI} profiles depend only on the variable X, which is the neutral fraction at the self-shielding radius r_{ss}. The radius is in physical unit for the left panel and is normalized by r_{ss} for the right panel.

fraction at the radius r_{ss} where the cloud becomes self-shielding: $X \equiv x_{HI,0}(r_{ss})$. Here, r_{ss} is defined as the impact parameter where the column density is $N_{HI,0}(r_{ss}) = a_{\nu_L}^{-1} = 1.59 \times 10^{17}\,\mathrm{cm}^{-2}$ with both $x_{HI,0}$ and $N_{HI,0}$ computed without including the self-shielding correction. Using the approximation $X \ll 1$ and ignoring also any external cutoff in the isothermal gas density profile, one finds

$$X = \left[\frac{1.64\alpha_B N_{HI,0}}{0.76\pi\,\Gamma r_{ss}}\right]^{1/2} \quad . \tag{2}$$

Thus, the shape of the neutral fraction profile depends only on the product Γr_{ss}. It is easily shown that the self-shielding radius r_{ss} is proportional to $(A^2/\Gamma)^{1/3} \propto M^{4/9}/\Gamma^{1/3}$. For the four halo masses we use, $(10^9, 10^{10}, 10^{11}$, and $10^{12} M_\odot)$, and $\Gamma = 1.25 \times 10^{-12}\,\mathrm{s}^{-1}$, we find $r_{ss} = 1.3, 3.6, 9.9,$ and $27.6\,\mathrm{kpc}$, and $X = 1.8 \times 10^{-3}, 1.1 \times 10^{-3}, 6.3 \times 10^{-4}$, and 3.8×10^{-4}, respectively. The right panel of Figure 1 shows the neutral fraction profiles for these four cases as a function of r/r_{ss}.

This general shape of the neutral fraction profiles of self-shielding clouds ionized by the cosmic background can be simply understood as follows: the cloud becomes self-shielding at the radius where the total rate of recombinations balances the rate at which photons come into the cloud. Therefore, once a radius $\sim r_{ss}$ is reached where most photons with frequency near ν_L have been absorbed, the cloud becomes mostly neutral over a small range in radius, because the rate of recombinations required to balance the absorption of all the higher frequency photons is not much higher. The effect has been demonstrated before by Murakami & Ikeuchi (1990) and Petitjean,

Bergeron, & Puget (1992), and is analogous to the sharp edges of H I disks produced by self-shielding (Corbelli & Salpeter 1993). Since $a_{4\nu_L} \simeq a_{\nu_L}/64$, we conclude that for $X > 1/64$, some of the highest frequency photons will penetrate into the atomic region of the cloud (causing a residual ionization inside the atomic region), while for $X < 1/64$, all the photons have mean free paths small compared to r_{ss} once the cloud is mostly atomic, so the intensity of ionizing photons suddenly drops to zero and there is a sharp transition to a completely atomic gas.

Figure 2 shows the predicted distribution of H I column densities, $f(N_{HI})$, when random lines of sight intersect the four model gas clouds (obtained by requiring $f(N_{HI})\, dN_{HI} \propto r\, dr$, where $N_{HI}(r)$ is found by integrating the hydrogen density times the neutral fraction in Fig. 1 over lines of sight at impact parameter r). The transition to atomic gas causes a feature in the distribution, with a hump appearing at column density $N_{HI} \sim N_{HI,0}\, X^{-1}$.

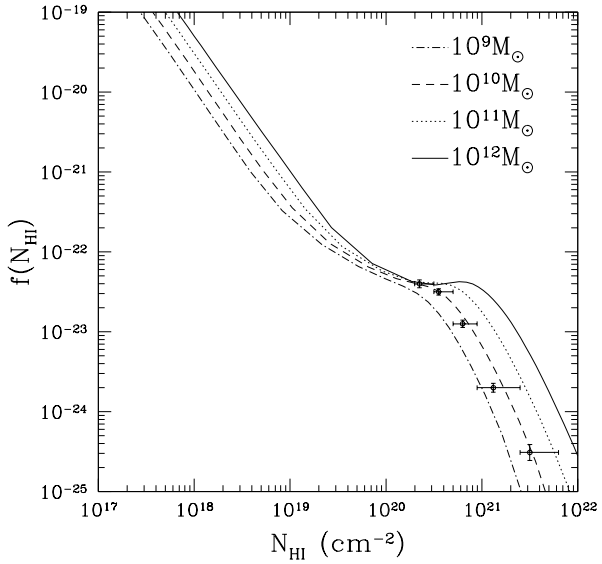

Fig. 2.— The probability distribution of the neutral hydrogen column density for different halo masses. Each curve is normalized so that the total probability of intersecting the halo within the virial radius is unity. Data points are from Storrie-Lombardi & Wolfe (2000) with a vertical shift.

Superposed on our curves, we reproduce a recent compilation of the column density distribution of known damped Lyα systems, from Storrie-Lombardi & Wolfe (2000). The points seem to fit best the curve for the $10^{10} M_{\odot}$ halo (notice that the points can be arbitrarily shifted vertically). In particular, the point at the lowest column density suggests a shallower slope of the distribution. This is a marginal indication that the feature predicted by the self-shielding effect may have been detected. If so, the value of X that is inferred is $X \simeq 1.1 \times 10^{-3}$, which for our adopted value of the photoionization rate Γ, corresponds to $r_{ss} \simeq 3.6\,\mathrm{kpc}$. We caution, however, that the predicted shape depends on the assumed total gas density profile, which we have taken to be singular isothermal.

4. DISCUSSION

We have shown that self-shielding should cause a sharp transition from an ionized to an atomic medium in any gas cloud photoionized by the external cosmic background. The expected absence of photons above frequency $4\nu_L$ due to He II absorption makes that transition even sharper once the neutral fraction has been increased by a factor 64 by self-shielding. This produces a hump in the column density distribution. The column density at which the hump occurs measures the quantity Γr_{ss}.

Most damped Lyα systems are likely to be photoionized by the external cosmic background. In fact, since their rate of occurrence is about one fourth per unit redshift at $z \sim 3$ (Storrie-Lombardi, McMahon, & Irwin 1996), and the mean free path of ionizing photons is $\Delta z \simeq 1$ (Miralda-Escudé & Ostriker 1990), it is easily shown that if all the sources of the cosmic ionizing background were embedded inside damped Lyα systems, then the local source in any such system would contribute about the same flux as the external background on average. It is much more likely that any sources associated with typical damped Lyα systems do not contribute significantly to the cosmic background.

The results for the column density distribution presented by Storrie-Lombardi & Wolfe (2000) suggest a possible detection of the self-shielding effect, which would imply a radius $r_{ss} \simeq 3.6\,\mathrm{kpc}$ for $\Gamma = 1.25 \times 10^{-12}\,\mathrm{s}^{-1}$. This represents a measurement of the size of the clumps in damped Lyα systems. Even though our calculation is for a spherical, isolated cloud, a system of randomly located clumps would produce a similar column density distribution depending on the radius of the clumps, as long as each clump is illuminated by the ionizing background with an optical depth $\lesssim 1$ along a large fraction of directions. This should be correct since the typical number of intersected clumps identified in the metal absorption lines is not very large.

The typical size of damped Lyα systems inferred from CDM models where all halos with $V_c \geq 40\,\mathrm{km\,s}^{-1}$ give rise to the absorption systems is 1 to 10 kpc (e.g., Katz et al. 1996; Gardner et al. 1997; McDonald & Miralda-Escudé 1999). Hydrodynamic cosmological simulations show that, at redshift $z \sim 2-4$, for halos more massive than $\sim 10^{11} M_\odot$, the projected distance of DLAs to the center of the nearest galaxy is around 10 kpc (Gardner et al. 2001). Since the clump size we infer is about the same, this suggests that the multiple metal absorption lines do not arise from highly overdense clumps, but from mild density fluctuations in gaseous halos. If there were highly overdense clumps, their small self-shielding radii would produce a column density distribution with a less pronounced hump at lower column density than the curves in Figure 2. The appearance of individual absorption lines in the spectra of Mg II and other metal lines might be deceiving, and could be due to a continuous medium, where the Mg II density is highly sensitive to the gas density due to photoionization and self-shielding effects.

Nevertheless, a number of caveats must be borne in mind in interpreting the observed column density distribution as a measurement of Γr_{ss}. In reality, there should be a distribution of clump sizes, and differences from a simple spherical geometry would introduce additional variations, which

would smooth the shape of the distribution predicted in Figure 2. Furthermore, the density profile of the gas cloud can be different from what we assume here. A fully three-dimensional calculation of self-shielding in a hydrodynamic simulation of galaxy formation would be highly desirable for a more robust interpretation of the observations of damped Lyα systems.

Finally, we mention that once the size of the clumps is known, their column densities can be used to infer their gas mass, and the temperature required to have a cloud in hydrostatic equilibrium (see Corbelli, Salpeter, & Bandiera 2001). Using a typical column density $N_H \sim 3 \times 10^{20}\,\mathrm{cm}^{-2}$ for a clump, and a radius $r_{ss} \simeq 3.6\,\mathrm{kpc}$, a gas mass of $M_g \simeq 1.6 \times 10^8 M_\odot$ is inferred for the self-shielded region. In the absence of dark matter, the temperature in hydrostatic equilibrium is $T \simeq GM_g m_H / k r_{ss} \simeq 2.3 \times 10^4\mathrm{K}$. Since this is near the expected temperature in photoionization equilibrium, this would imply that the gas clumps in damped systems do not contain a lot of dark matter. However, this conclusion is altered if the gas temperature is higher due to shock heating or turbulent motions are important.

This work was supported in part by NSF grant NSF-0098515.

REFERENCES

Corbelli, E., & Salpeter, E. E. 1993, ApJ, 419, 104

Corbelli, E., Salpeter, E. E., & Bandiera, R. 2001, ApJ, 550, 26

Gardner, J. P., Katz, N., Hernquist, L., & Weinberg, D. H. 1997, ApJ, 484, 31

Gardner, J. P., Katz, N., Hernquist, L., & Weinberg, D. H. 2001, ApJ, 559, 131

Haardt, F., & Madau, P. 1996, ApJ, 461, 20

Haehnelt, M. G., Steinmetz, M., & Rauch, M. 1998, ApJ, 495, 647

Haehnelt, M. G., Steinmetz, M., & Rauch, M. 2000, ApJ, 534, 594

Katz, N., Weinberg, D. H., Hernquist, L., & Miralda-Escudé, J. 1996, ApJ, 457, L57

Lanzetta, K. M., Wolfe, A. M., Turnshek, D. A., Lu, L., McMahon, R. G., & Hazard, C. 1991, ApJS, 77, 1

López, S. Reimers, D., Rauch, M., Sargent, W. L. W., & Smette, A. 1999, ApJ, 513, 598

McDonald, P., & Miralda-Escudé, J. 1999, ApJ, 519, 486

Miralda-Escudé, J., & Ostriker, J. P. 1990, ApJ, 350, 1

Murakami, I., & Ikeuchi, S. 1990, PASJ, 42, L11

Osterbrock, D. E. 1989, Astrophysics of Gaseous Nebulae and Active Galactic Nuclei (Mill Valley: University Science Books)

Padmanabhan, T. 1993, Structure Formation in the Universe (Cambridge: Cambridge Univ. Press)

Petitjean, P., Bergeron, J., & Puget, J. L. 1992, 265, 375

Prochaska, J. X., & Wolfe, A. M. 1997, ApJ, 474, 140

Prochaska, J. X., & Wolfe, A. M. 1998, ApJ, 507, 113

Rauch, M., Sargent, W. L. W., & Barlow, T. 1999, ApJ, 515, 500

Spitzer, L., Jr. 1978, Physical Processes in the Interstellar Medium (New York: Wiley)

Storrie-Lombardi, L. J., & Wolfe, A. M. 2000, ApJ, 543, 552

Storrie-Lombardi, L. J., McMahon, R. G., & Irwin, M. J., 1996, MNRAS, 282, 1330

Tajiri, Y., & Umemura, M. 1998, ApJ, 502, 59

Verner, D. A., & Ferland, G. J. 1996, ApJS, 103, 467

Wolfe, A. M., Lanzetta, K. M., Foltz, C. B., & Chaffee, F. H. 1995, ApJ, 454, 698